The Cryosphere, 9, 613–629, 2015
www.the-cryosphere.net/9/613/2015/
doi:10.5194/tc-9-613-2015

The Cryosphere
Open Access

Configuration of the Northern Antarctic Peninsula Ice Sheet at LGM based on a new synthesis of seabed imagery

C. Lavoie[1,2], E. W. Domack[3], E. C. Pettit[4], T. A. Scambos[5], R. D. Larter[6], H.-W. Schenke[7], K. C. Yoo[8], J. Gutt[7], J. Wellner[9], M. Canals[10], J. B. Anderson[11], and D. Amblas[10]

[1]Istituto Nazionale di Oceanografia e di Geofisica Sperimentale (OGS), Borgo Grotta Gigante, Sgonico, 34010, Italy
[2]Department of Geosciences/CESAM, University of Aveiro, Aveiro, 3810-193, Portugal
[3]College of Marine Science, University of South Florida, St. Petersburg, Florida 33701, USA
[4]Department of Geosciences, University of Alaska Fairbanks, Fairbanks, Alaska 99775, USA
[5]National Snow and Ice Data Center, University of Colorado, Boulder, Colorado 80309, USA
[6]British Antarctic Survey, Cambridge, Cambridgeshire, CB3 0ET, UK
[7]Alfred Wegener Institute, Helmholtz Centre for Polar and Marine Research, Bremerhaven, 27568, Germany
[8]Korean Polar Research Institute, Incheon, 406-840, Republic of Korea
[9]Department of Earth and Atmospheric Sciences, University of Houston, Houston, Texas 77204, USA
[10]Departament d'Estratigrafia, Paleontologia i Geociències Marines/GRR Marine Geosciences, Universitat de Barcelona, Barcelona 08028, Spain
[11]Department of Earth Science, Rice University, Houston, Texas 77251, USA

Correspondence to: C. Lavoie (clavoie@ua.pt) or E. W. Domack (edomack@usf.edu)

Received: 13 September 2014 – Published in The Cryosphere Discuss.: 15 October 2014
Revised: 18 February 2015 – Accepted: 9 March 2015 – Published: 1 April 2015

Abstract. We present a new seafloor map for the northern Antarctic Peninsula (AP), including swath multibeam data sets from five national programs. Our map allows for the examination and interpretation of Last Glacial Maximum (LGM) paleo-ice-flow paths developed on the seafloor from the preservation of mega-scale glacial lineations, drumlinized features, and selective linear erosion. We combine this with terrestrial observations of flow direction to place constraints on ice divides and ice domes on the AP continental shelf during the LGM time interval. The results show a flow bifurcation as ice exits the Larsen B embayment. Flow emanating off the Seal Nunataks (including Robertson Island) is directed toward the southeast, then eastward as the flow transits toward the Robertson Trough. A second, stronger "streaming flow" is directed toward the southeast, then southward as ice overflowed the tip of the Jason Peninsula to reach the southern perimeter of the embayment. Our reconstruction also refines the extent of at least five other distinct paleo-ice-stream systems that, in turn, serve to delineate seven broad regions where contemporaneous ice domes must have been centered on the continental shelf at LGM. Our reconstruction is more detailed than other recent compilations because we followed specific ice-flow indicators and have kept tributary flow paths parallel.

1 Introduction

The reconstruction of paleo-ice sheets/stream-flow directions depends first upon an accurate assessment of ice domes, ice divides, and outlet flow paths (Andrews, 1982). Studies of the configuration of the Antarctic Peninsula Ice Sheet (APIS) during the Last Glacial Maximum (LGM; time interval ∼23–19 kyr BP) suggest that the grounded ice reached the continental-shelf break (e.g., Larter and Barker, 1989; Banfield and Anderson, 1995; Larter and Vanneste, 1995; Wellner et al., 2001; Canals et al., 2002; Evans et al., 2005; Heroy and Anderson, 2005; Amblas et al., 2006; Wellner et al., 2006; Simms et al., 2011). The seafloor of the Antarctic Peninsula (AP) continental shelf is characterized by over-

deepened troughs and basins where mega-scale glacial lineations (MSGLs) (Clark, 1993; Clark et al., 2003) and large-scale flow line bedforms such as glacial flutes, mega-flutes, grooves, drumlins, and crag-and-tails provide geomorphic evidence for former regional corridors of fast-flowing ice and drainage directions of the APIS on the continental shelf. Also of importance is their synchroneity as the ice flows change during the ice sheet evolution from ice sheet to ice stream to ice shelf (Gilbert et al., 2003; Dowdeswell et al., 2008).

Our capability to image specific flow directions and styles on the Antarctic continental shelf is critical to any glacial reconstruction because they help us to understand the present and future ice sheet's behavior. Recently, Livingstone et al. (2012) published an inventory of evidence for paleo-ice streams on the continental shelf of Antarctica at LGM. Their reviews are in agreement with previous studies and highlight that the western (Pacific) AP continental shelf is characterized by preferred regional ice-flow pathways on the middle shelf through cross-shelf troughs connected to major flow paths on the outer shelf (e.g., Evans et al., 2004; Heroy and Anderson, 2005). On the other side, the eastern (Weddell Sea) AP continental shelf is less well defined but characterized by multiple deep tributaries on the inner shelf that converge in shallow troughs on the mid- to outer shelf (e.g., Evans et al., 2005). Nevertheless, our knowledge on the APIS configuration at the LGM time interval, such as paleo-flow paths in the Larsen B embayment, is limited and particularly relevant to the ice sheet reconstruction, where the broad continental shelf served as a platform for extension of the glacial systems that spilled off the Detroit and Bruce Plateau ice caps. In fact, the AP is believed to have experienced the largest percentage change in areal extent of glacial cover of any sector of the Antarctic margin through the last glacial cycle (i.e., MIS stages 2 to 1). For instance, our reconstruction shows that the current APIS covers $\sim 23\,\%$ of the total area of grounded ice coverage at LGM. The APIS system in particular is a significant bellwether system in the evolution of the Antarctic Ice Sheet because it is

1. the one system today that is most closely tied to surface-driven ablation and accumulation change (Rebesco et al., 2014) rather than driven mainly by oceanographic change such as in the West Antarctic Ice Sheet, having equilibrium lines above sea level (a.s.l.) as a consequence of significantly warm summer temperatures;

2. exposed to a contrasting oceanographic regime of cold and warm water on the eastern and western sides, respectively; and

3. the most northern of the ice sheet systems and is exposed to southward excursions in westerly winds and the Antarctic Circumpolar Current.

In this paper, we examine and interpret the paleo-ice-flow directions of the APIS based on a new synthesis of single and swath bathymetry data and provide a comprehensive assessment of the flow paths, ice divides, and ice domes pertaining to the glacial history of the northern APIS at the LGM time interval. These ice divides can either be ice ridges or local ice domes with their own accumulation centers, which are ice divides with a local topographic high in the ice surface and flow emanating in all directions (although not necessarily equally). The shape of an ice dome may range from circular to elongated; elongated ridge-like ice domes are common amongst the present-day ice streams of West Antarctica. The spatial coverage of the bathymetric data is extensive (Fig. 1) and for this and the above reasons we focus on regional systems by dividing it into seven sectors. These include the (1) Larsen B embayment, (2) Larsen A and James Ross Island, (3) Joinville Archipelago Platform, (4) Bransfield Strait, (5) Gerlache–Croker–Boyd straits, (6) Palmer Deep and Hugo Island Trough, and (7) Biscoe Trough. First, we highlight the geomorphic features that define the specific flow paths at LGM and glacial tributaries across the inner to outer shelf. We combine this with terrestrial observations of flow direction to place constraints on ice divides and ice domes that controlled the APIS flow drainage and subsequent retreat history. Finally, we discuss the characteristics of the reconstructed northern APIS and its regional significance for ice sheet modeling.

2 Methods

2.1 Data sets

Extensive multibeam swath bathymetry data have been acquired from several regions including those recently uncovered by the collapse of the Larsen Ice Shelf system. Ice-flow directions within the Larsen B embayment are indicated by a series of interconnected (1) multibeam surveys beginning with a USAP program in 2000 and followed by the British Antarctic Survey (2002), additional USAP surveys (2001 and 2006), Alfred Wegener Institute, Helmholtz Centre for Polar and Marine Research surveys (2007 and 2011), Korea Polar Research Institute survey (KOPRI, 2013) under the LARISSA project, and (2) single-beam sonar data from USAP in 2005. Detailed observations of the seafloor morphology in the Larsen A embayment, the area surrounding James Ross Island and offshore from Joinville Archipelago were collected by the USAP program between 2000 and 2002, 2005 and 2007, and in 2010 and 2012, including work by the British Antarctic Survey (2002) and United Kingdom Hydrographic Office (2006–2008). The Bransfield Strait has been covered by the Spanish Antarctic program between 1991 and 1997, USAP program (1995–1997, 1999–2002, and 2005–2011), and United Kingdom Hydrographic Office (2006–2008, 2010 and 2012). The multibeam swath bathymetry data from the Gerlache–Croker–Boyd Strait, Palmer Deep and Hugo Island Trough, and Biscoe Trough

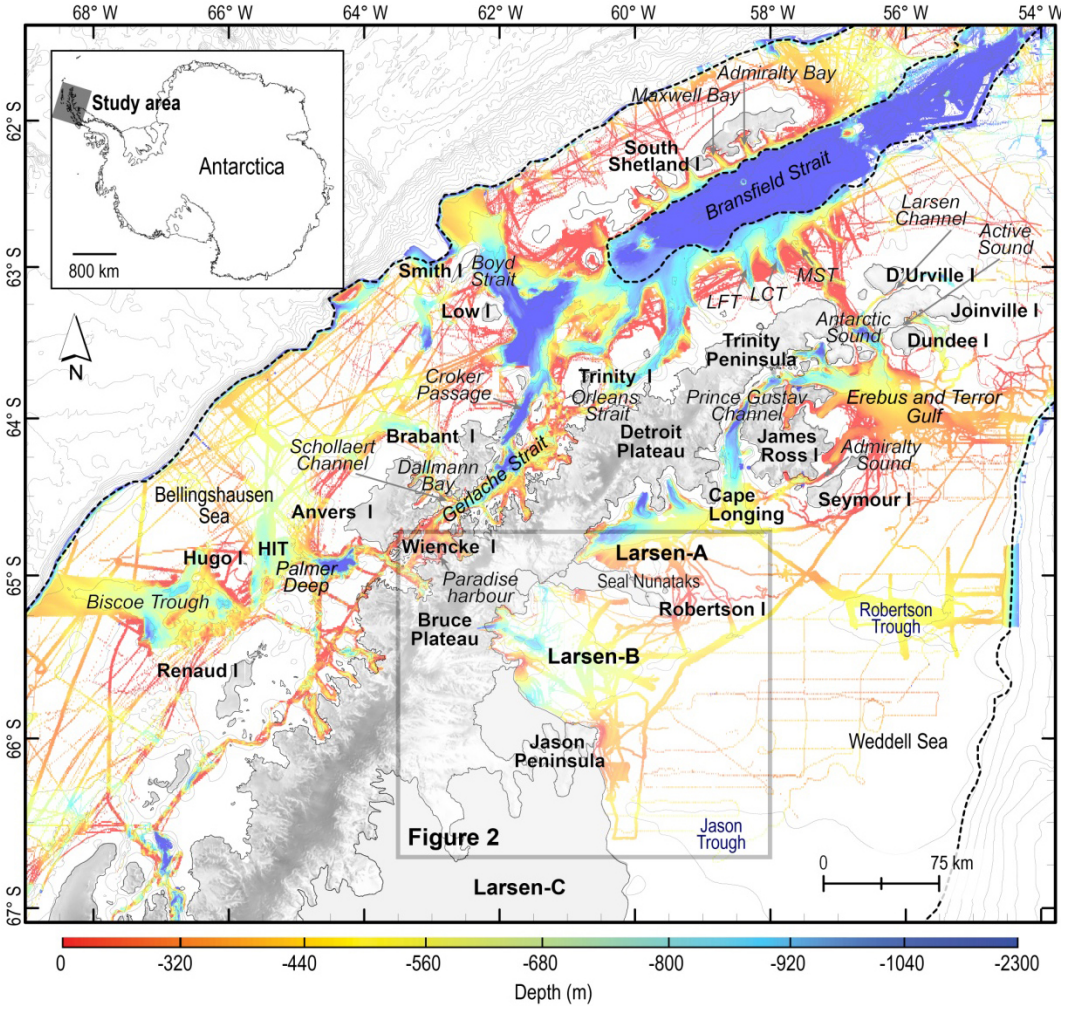

Figure 1. Location map and details of the swath bathymetry database, as compiled up to 2013, around the northern Antarctic Peninsula (AP). Offshore topography is gridded at 30 m. The shelf break is shown as a black dashed line. The gray box indicates the regions detailed in Fig. 2. The background image on land is from RAMP AMM-1 SAR Image 125 m Mosaic of Antarctica; the coastline is from the British Antarctic Survey (BAS; http://www.add.scar.org/); the bathymetry contour interval of 250 m is from IBCSO (Arndt et al., 2013). The inset shows the location of the northern AP in Antarctica. Abbreviations: HIT – Hugo Island Trough, LFT – Lafond Trough, LCT – Laclavere Trough, MST – Mott Snowfield Trough.

are from the USAP program (1995–1997, 1999–2002, and 2005–2012), the Spanish Antarctic program in 1996–1997 and 2001–2002, and KOPRI (2013). The data set was gridded at a cell size of 30 m × 30 m and analyzed with illumination at variable azimuths. The high-resolution seabed images were gridded at a cell size of 25 m × 25 m. Additional single-beam sonar data from NOAA National Geophysical Data Center Marine Trackline Geophysical database (http://ngdc.noaa.gov/mgg/geodas/trackline.html) were used to support the delineation of the continental-shelf ice domes.

2.2 Bedform mapping

We assume that our flow line reconstructions over sedimentary deposits are contemporaneous to the LGM time interval and that observed seafloor lineations over resistant substrate were carved last by the APIS at LGM, although formation of the latter may derive from time-integrated glacial processes (e.g., Nývlt et al., 2011). While it is possible that some portion of the preserved flow line features we examine are representative of the "death mask" state of the APIS (i.e., Wellner et al., 2006) rather than the mature LGM stage of the system, we suggest that this in general is not the case. We base this hypothesis upon specific observations and assumptions that include

1. only slight modification of flow trajectory as preserved along recessional grounding zones (i.e., Evans et al., 2005, Fig. 7), and such flow relationships are easily resolved;

2. a general shelf slope gradient that does not, except very locally, provide significant reversal in relief to have influenced evolving flow paths as ice would have thinned (drawn-down) and receded toward the coast;

3. clear association of converging flow paths from areas that would have provided divergent flow during stages of retreat (i.e., as from shelf ice domes).

From the observed seafloor lineations, we establish a central flow line at the root of each tributary glacier adjacent to areas of reasonable coverage in the multibeam data. We preserved these central flow lines by forcing tributary contributions to remain parallel and consistent with observed seafloor lineations. In this way converging flow can be evaluated more easily than by using "idealized" single-line flow arrows (as has been done on previous reconstructions). The number of lines in a given flow path is defined by the number of tributaries and is only a visual approximation of the ice discharge for that flow path. In some cases, ice flow across the seafloor diverged around obstacles but remained parallel within the larger confining troughs or fjords. Small-scale basal-flow divergence patterns such as these were not preserved in our reconstruction.

The orientation of the bedrock striations at Cape Framnes and Foyn Point (Larsen B embayment; Fig. 2) were measured with a Brunton Compass, corrected for regional declination, and compared to visual data of large-scale bedrock fluting from overflights during 2010 (USAP-ship-based helicopters during LARISSA NBP10-01 cruise).

2.3 Ice volume estimation and assumptions

We utilize two different algorithms to estimate volumes of the ice sheet, depending upon the type of system, streaming flow, or ice domes. The average depths along the flow paths are estimated from our swath bathymetry map and the International Bathymetric Chart of the Southern Ocean (IBCSO) map gridded at 500 m (Arndt et al., 2013). For the minimum volumes, we assume that the ice streams were lightly grounded until the shelf break or to the end of the defined flow path (except for Larsen B/Jason Trough), where the ice thickness must be about 10 % more than the average depth to prevent flotation (allowing the deepest areas to be subglacial lakes rather than full of ice). We assume a minimal surface slope (0.001) similar to the lowest sloping modern ice streams. For the maximum volumes, we assume that the ice was grounded to the continental-shelf break (except for Larsen B/Jason Trough). We assume the surface slope of the ice was steeper (0.005) but not too steep to exceed the nearby ice divide elevations. The real slope will depend on the geology. A softer more malleable bed would favor a lower profile ice stream, while a stiffer bed would lead to a slightly steeper profile. For the ice domes in this reconstruction, we use a radially symmetric Bodvarsson–Vialov model as presented in Bueler et al. (2005). This model assumes the shallow-ice approximation (no sliding bed) and Glen-type ice flow with a softness that depends on the average temperature. The model can directly predict the thickness as a function of distance from the dome center ($r = 0$) as

$$H(r) = \left(2^{(n-1)}\frac{\dot{b}}{\Gamma}\right)^{1/(2n+2)} (L^{1+1/n} - r^{1-1/n})^{n/(2n+2)}, \quad (1)$$

$$\Gamma = \frac{2A(\rho g)^n}{n+2}, \quad (2)$$

where H is the ice thickness, $\dot{b}$ is the accumulation rate, L is the lateral extent of the ice dome, assuming it is circular, and $n = 3$ for typical Glen-type ice flow. Γ is a parameter that depends on the ice softness, A, which is temperature dependent, the density (ρ) of ice, and gravity (g). The specific values of A used are for warm ice $6.8^{e-15}\,\mathrm{s}^{-1}\,\mathrm{kPa}^{-3}$ and cold ice $4.9^{e-16}\,\mathrm{s}^{-1}\,\mathrm{kPa}^{-3}$ (Cuffey and Paterson, 2010). Because we lack specific data for LGM accumulation rate and ice temperature, we use our best guesses to bound the ice thicknesses and volumes as follows. We assume that the same strongly orographic precipitation occurred during LGM interval as today and the ice temperature was around 0 °C (mostly temperate) for the western AP domes and averaging −20 °C for the domes located on the eastern side. For the modern AP, the western side has higher average temperatures than the eastern side, suggesting that, in the past, the ice domes on the western side were warmer on average than the eastern side. We based the minimum and maximum dome volumes on a low-end and high-end approximation of the accumulation rates, respectively. In these accumulation rate assumptions, we took into account that some domes are more exposed to the prevailing storm direction and some will be in the lee, resulting in higher or lower accumulation rates. Also, we take the geologically defined aerial dome extent and assume a dome base of circular area that has the same area as the geologically defined dome. The approximation of a circular dome with the same average radius as the estimated bathymetric features will introduce additional source of uncertainty into the volume estimates. This circular dome assumption may overestimate volume if the real feature is a oval ridge shape, but it may underestimate the volume if the dome is bounded by thick ice streams. Without more constraints, we feel the uncertainties due to the circular dome assumption are small compared to the uncertainties due to the accumulation rate and temperature assumptions.

3 Results

3.1 Larsen B embayment

The major collapse of the Larsen B Ice Shelf in 2002 (Scambos et al., 2003), unprecedented in the Holocene history of

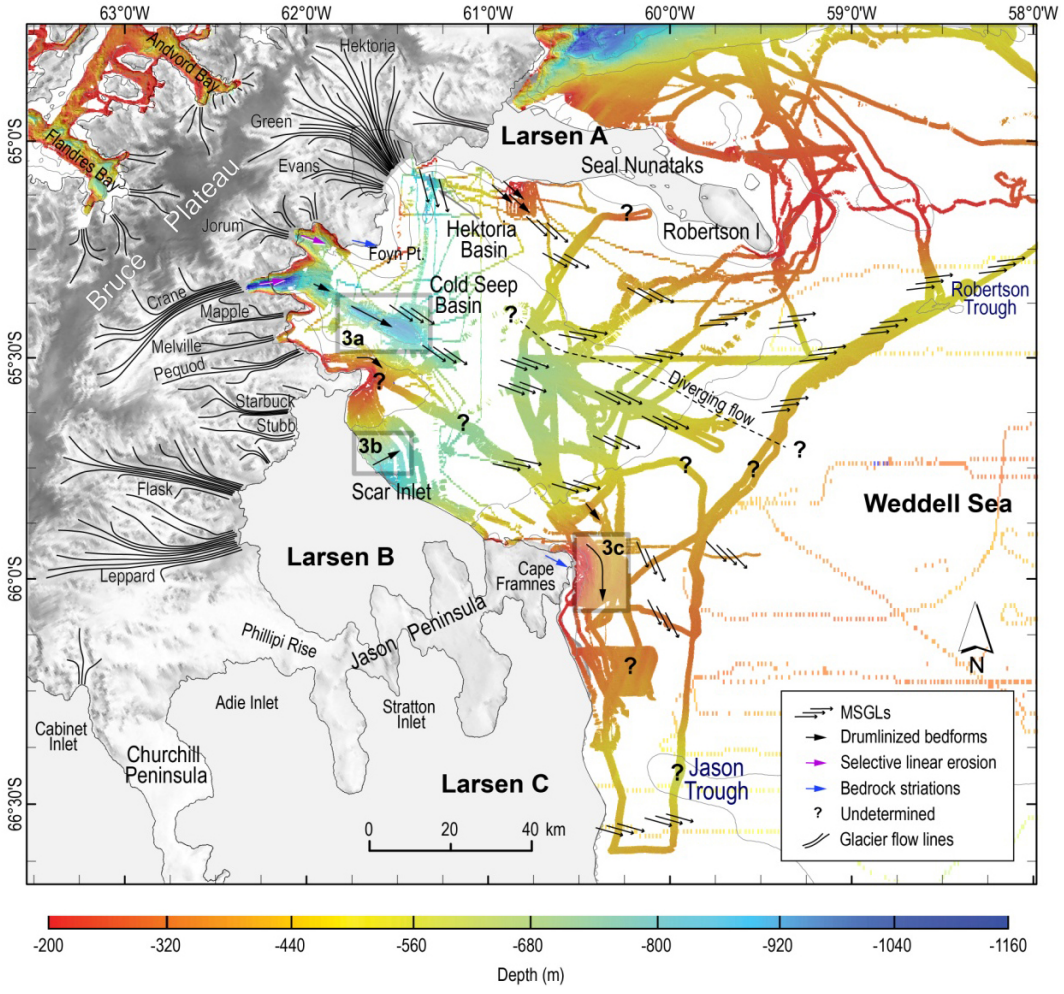

Figure 2. Details of seabed morphology in Larsen B embayment associated with paleo-flow-line trajectories based on examination of swath bathymetry imagery of the seafloor. Distinct flow trajectories split the Larsen B embayment into two outlets by ice-flow bifurcation. The bathymetry contour interval of 250 m is from IBCSO (Arndt et al., 2013). The gray boxes show the regions detailed in Fig. 3. For location see Fig. 1.

this glacial system (Domack et al., 2005; Curry and Pudsey, 2007), has provided a unique opportunity for seafloor mapping. This work reveals a far more detailed flow pattern in Larsen B embayment than that inferred by general orientation of bathymetric troughs derived from sparse swath or single-line bathymetric data. Such earlier approaches suggested that all Larsen B ice flowed out toward the Robertson Trough (e.g., Evans et al., 2005; Davies et al., 2012; Livingstone et al., 2012).

By using a more detailed analysis of flow indicators available from the swath data, we now recognize two distinct flow trajectories that split the Larsen B embayment into two outlets (Fig. 2). The first relates to the attenuated drumlinized bedforms and highly attenuated MSGLs observed in the northern perimeter of the Larsen B embayment. The ice flow emanating off the Seal Nunataks and Robertson Island directed flow toward the southeast and then eastward as the flow transits toward the Robertson Trough, a feature that connects Larsen A and B (Evans et al., 2005). This flow pattern extends across relatively shallow depths of less than 500 m and was probably fed by small tributary confluence.

In contrast, the southern perimeter is marked by stronger "streaming flow" indicators fed by large tributaries draining the APIS, including the Crane Glacier and most likely the Evans, Green, and Hektoria glaciers. The well-defined drumlinized bedforms with crescentic scour and MSGLs indicate that ice flow was funneled into the Cold Seep Basin (Fig. 3a) and moved toward the southeast from the interior. From the southern edge of Scar Inlet (Larsen B Ice Shelf), the swath bathymetric map shows evidence of a northeastward flow (Fig. 3b) that shifted in a downstream direction toward the southeast, thus convergent with the flow streaming from the Cold Seep Basin corridor. The Scar Inlet ice stream system was fed by the tributaries of the Starbuck, Flask, and Leppard

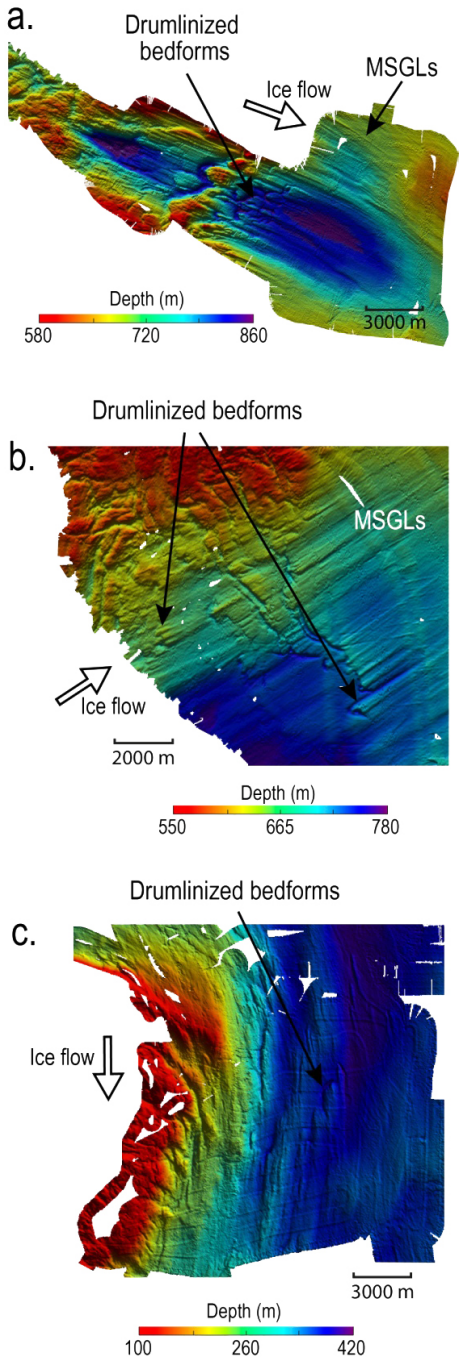

Figure 3. Close-up on the seabed morphology and swath bathymetry perspective views. The location of **(a)**–**(c)** is presented in Fig. 2. Offshore topography is gridded at 25 m and shown with a vertical exaggeration of X3. **(a)** Bathymetry image shows the Cold Seep Basin region with drumlinized bedforms and mega-scale glacial lineations (MSGLs) associated with a paleo-ice-flow direction, **(b)** Scar Inlet, and **(c)** Cape Framnes, south of the Jason Peninsula. The paleo-ice-flow direction is indicated by the white arrows.

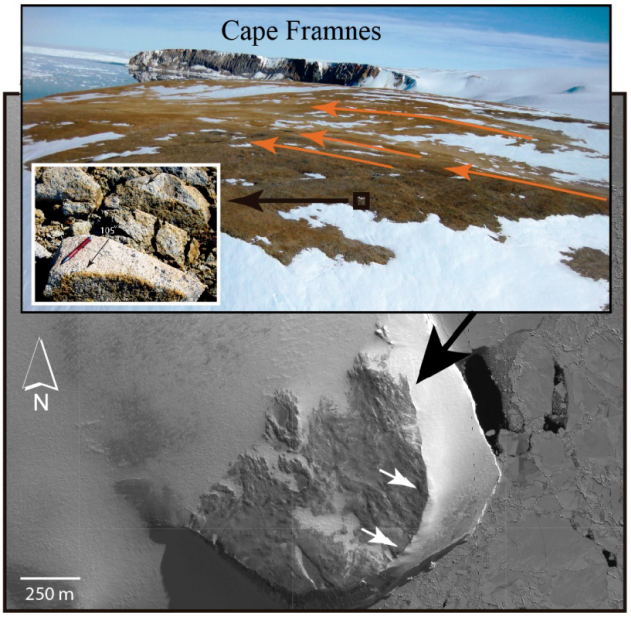

Figure 4. Photograph from Cape Framnes showing bedrock striations and flute orientations ESE in agreement with the southward flow orientation observed on the seafloor (this study). The location of the photograph and its aspect are indicated by the black arrow on the Landsat Scenes LIMA. The insets show an isolated bedrock rib, its location on the landscape, and the flow direction of striations and bedrock flutes (orange and white arrows) in each case (figure modified from a map compiled by Spences Niebuhr, Polar Geospatial Center).

glaciers. Our flow line bedform compilation suggests that the southeastward flow in the southern part of the Larsen B embayment changed to a southward direction with ice overflowing the tip of the Jason Peninsula, offshore the northern region of the Larsen C Ice Shelf (Figs. 2 and 3c), to reach the Jason Trough. This southward flow orientation is supported by east-southeast bedrock striations and flute orientations at Cape Framnes, Jason Peninsula (Fig. 4), that are in similar orientation to the flow indicators found directly offshore.

Finally, the southernmost swath bathymetry data at the edge of the northern Larsen C Ice Shelf indicate a southeastward ice-flow orientation on a seafloor deeper than 400 m. Recent seismic reflection soundings close to the northern ice shelf front and inward show a uniform water cavity thickness beneath the ice shelf of around 220 to 240 m (Brisbourne et al., 2014).

3.2 Larsen A and James Ross Island

Our mapped flow pattern of the Larsen A and James Ross Island sector differs only in fine detail to those of earlier reconstructions (e.g., Evans et al., 2005; Johnson et al., 2011; Davies et al., 2012). The data show the establishment of two major outlets: the Robertson Trough system and the Erebus–Terror system (Fig. 5). The Robertson Trough system col-

lected flow out of the Larsen A, southern Prince Gustav Channel, and portions of Admiralty Sound. The ice flowed from the Larsen A, derived mainly from the Detroit Plateau (AP), toward the south and then east. It then coalesced with the southern Prince Gustav Channel flow across the shelf toward the southeast and finally directly east (Pudsey et al., 2001; Gilbert et al., 2003; Evans et al., 2005). On the outer shelf the ice flow coalesced with the northern perimeter of the Larsen B flow to form a major ice-flow trend in the Robertson Trough.

The Erebus–Terror system captured flow out of the northern Prince Gustav Channel, Antarctic Sound, and Admiralty Sound. The northern Prince Gustav Channel shows evidence of a main eastern flow direction fed by tributaries from ice caps on Trinity Peninsula and James Ross Island before coalescing with the Antarctic Sound and Admiralty Sound flows into the Erebus and Terror Gulf to reach the shelf break. Flow within the Prince Gustav Channel was separated from the south Larsen A system by an ice divide that extended from the Detroit Plateau across to James Ross Island (Camerlenghi et al., 2001). Recent observations and cosmogenic isotope exposure age dating on erratic boulders on James Ross Island by Glasser et al. (2014) suggest that the ice divide that crossed the central Prince Gustav Channel may only have been developed during the post-LGM recession.

3.3 Joinville Archipelago platform

The platform surrounding the northernmost extension of the AP terrain (D'Urville, Joinville, and Dundee Islands) has very limited multibeam coverage. Only two distinctive troughs have been imaged and flow lines are conjectural and defined (as in earlier approaches) by recognition of bathymetric troughs. Portions of the flow out of the Larsen Channel, between D'Urville Island and Joinville Island, and out of Active Sound between Joinville Island and Dundee Island ran in a southwestern direction, coalescing with the Antarctic Sound flow to the Erebus–Terror system. The other portion shows evidence of east and southeast flows. South of Joinville Island, the multibeam data imaged drumlin-like features indicating that ice was grounded on the Joinville Plateau, suggesting that the APIS extended across the shelf (Smith and Anderson, 2011; their Fig. 6).

3.4 Bransfield Strait

The continental shelves off the Trinity Peninsula (e.g., Lawver et al., 1996; Canals et al., 2002) and the South Shetland Islands (Simms et al., 2011) reveal paths of paleo-ice streams that drained into the Bransfield Strait. This narrow and deep (greater than 1000 m) strait was formed by rifting, actively spreading for the past 4 million years in response to subduction in the South Shetland Trench (Barker, 1982). Based on seafloor evidence, the grounded ice flow along the Bransfield Basin's perimeter transitioned to an ice shelf in deeper water (floating glacier ice that was not in contact with the seafloor). This system must have been confined to the Bransfield Basin between tributary flow out of the Orleans Strait, off the Trinity Peninsula, and the South Shetland Islands (Figs. 5 and 6). As indicated by the curvature of bedforms on the surface of the grounding zone fans (i.e., mouths of both Maxwell and Admiralty bays) and major troughs (i.e., Lafond, Laclavere, and Mott Snowfield Troughs) that extend into Bransfield Strait, flow of the ice shelf was conjectured to involve a northeastern direction more or less parallel to the trend of the basin (Canals et al., 2002; Willmott et al., 2003). Outlets in the eastern portions of the basin are even less well defined but must have involved partitioned grounded flow out across the northern end of the South Shetland Platform (just northeast of King George Island), out beyond Elephant Island, and into the Powell Basin (Fig. 6). According to the swath bathymetry data, it is likely that there was a small ice dome over Elephant Island providing a plug to the northeast-flowing Bransfield Ice Shelf system.

3.5 Gerlache–Croker–Boyd straits

In the Gerlache–Croker–Boyd straits, the streaming ice flow is confined in a spectacular bundle structure 100 km long and flowing to the north-northwest (Canals et al., 2000). Almost the entire ice drainage out of the Gerlache Strait was funneled through the Croker Passage, which included glaciers draining the eastern side of Anvers and Brabant islands and the western flank of the Bruce Plateau (Domack et al., 2004; Evans et al., 2004). These tributary systems converged at various depths (submarine hanging valleys) where fjord valleys joined the Gerlache Strait and the Croker Passage. This, along with the large number of tributaries, requires considerable constriction of parallel arrangement of flow lines within the Croker Passage and Boyd Strait outlet path (Fig. 5). Near, near the shelf break the grounding line system shows a spread of flow trajectories out toward the shelf break (Canals et al., 2003; their Fig. 2b).

3.6 Palmer Deep and Hugo Island Trough

The outflow from the Palmer Deep and Hugo Island Trough is one of the three major tributary systems that terminate as an outlet system along the western AP continental-shelf edge (Fig. 5). This flow system was delineated first by Pudsey et al. (1994), then by Vanneste and Larter (1995), and later outlined in detail by Domack et al. (2006). The systems include tributary glaciers from the Graham Land Coast between 65 and 66° S and ice which flowed out of Dallmann Bay around the northeast corner of Anvers Island (Fig. 5). Along the Graham Land Coast the ice flow emanating from the fjords directed flow to the northeast, coalescing with the Palmer Deep ice flow in Hugo Island Trough, and crossed the mid-shelf in a northern direction to the outer shelf (Domack et al., 2006). On the outer shelf the ice flow coalesced with the Dallmann

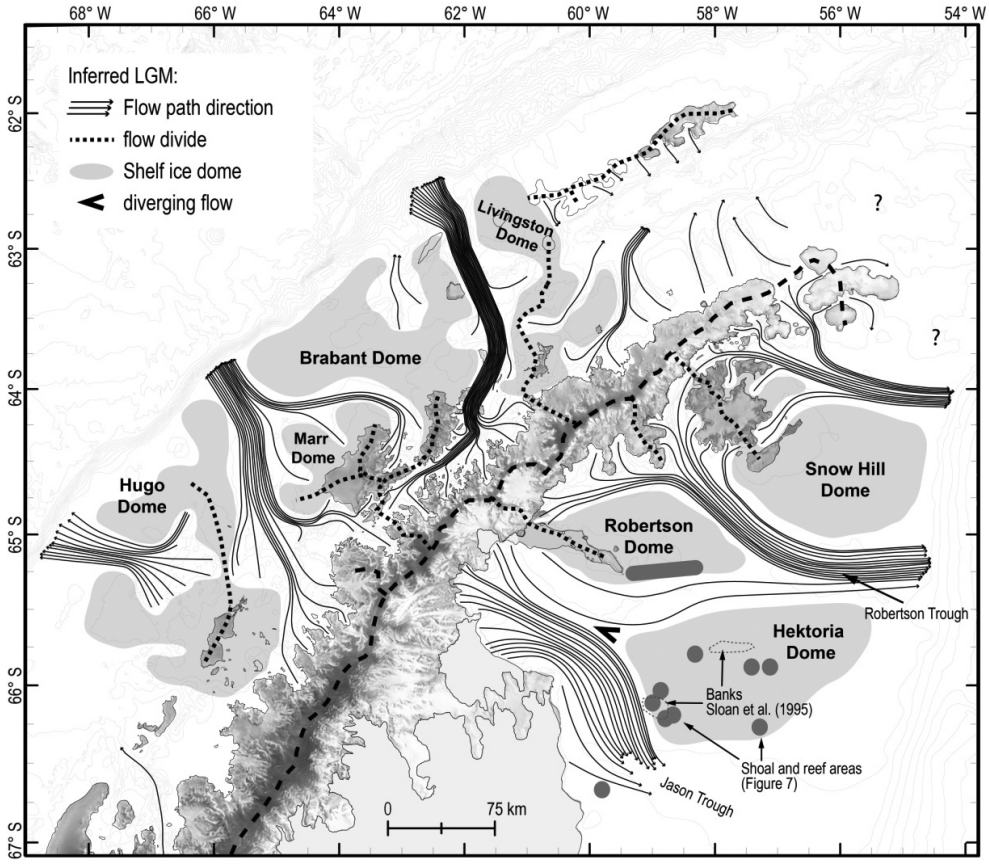

Figure 5. Inferred paleo-ice-flow directions and continental-shelf ice domes around the northern AP continental shelf at LGM showing ice divides (black short-dashed lines), shelf ice domes (gray areas), and the bifurcating flow in the Larsen B embayment. The modern divide along the AP (black dash line) is probably not at the same location of the LGM divide, but it is close. Also identified are the topographic banks by Sloan et al. (1995) and the shoal and reef areas of Fig. 7. The bathymetry contour interval of 250 m is from IBCSO (Arndt et al., 2013).

Bay flow that runs out around the north end of Anvers and Brabant islands.

3.7 Biscoe Trough

The cross-shelf Biscoe Trough system consists of three flow branches with overly deepened troughs up to 800 m depth, a topographic ridge of 300 m high crosses the main branch of the Biscoe Trough system in a southwest and northeast direction, and a smoother surface toward the shelf edge at 400–500 m depth (Canals et al., 2003; Amblas et al., 2006). The flow line bedforms show a general converging westward flow directions toward the shelf edge. The Biscoe Trough system also shows a spread of flow trajectories out toward the shelf break. This system was fed by ice flow primarily off Renaud Island archipelago but notably also contains indications of ice flow off mid- to outer shelf banks, with a distinct flow divide between the Biscoe Trough and Palmer Deep and Hugo Island Trough systems, and south along the trend defined by Hugo Island.

4 Interpretation and discussion

Based on the above observations we recognized six major outlets for paleo-ice-stream drainage off the APIS during the LGM and refined the locations of their ice divides (Fig. 5). In addition, the patterns revealed by our flow direction reconstruction indicate the locations and areal dimensions of at least seven major ice domes centered on the middle to outer AP continental shelf. Below we focus on a comprehensive interpretation of the new seabed morphology and discuss the regional implications regarding flow paths, ice divides, and ice domes.

4.1 Flow bifurcation in Larsen B embayment

Our observations of streamed bedforms in the Larsen B embayment indicate that the modern glaciers (i.e., Crane, Leppard, and Flask Glaciers) were not tributaries of the Robertson mid-outer shelf paleo-ice stream as previously interpreted by Evans et al. (2005) and highlighted in previous reviews (e.g., Davies et al., 2012; Livingstone et al., 2012).

Table 1. Reef and shoal areas in the northwestern Weddell Sea*.

Latitude	Longitude	Notes
65.237° S 65.183° S	59.251° W to 58.213° W	"Robertson reef": 49 km long, bearing numerous 005° high points, shallow depth (est. ∼ 100 m depth)
66.912° S 66.813° S	60.133° W to 59.468° W	"Bawden reef": extending 34 km from southern end of ice rise, arcuate, bearing numerous 020° high points, shallow depth (est. ∼ 100 m depth)
66.174° S 66.177° S 66.025° S	58.968° W W 58.721° W E 58.806° W N	"Jason shoals": 12 × 18 km region, 3–4 high points, shallow depth at west end (est. 100–150 m depth)
65.784° S	58.237° W	"Hektoria 1 shoal", single point (est. > 150 m depth)
65.849° S	57.276° W	"Hektoria 2 shoal", single point (est. > 150 m depth)
65.692° S	56.956° W	"Hektoria 3 shoal", single point (est. > 150 m depth)
66.292° S	56.975° W	"Hektoria 4 shoal", single point (est. > 150 m depth)

* Based on sea ice and small iceberg strand sites and winter sea ice fracture loci seen in MODIS image data archived at http://nsidc.org/data/iceshelves_images/index_modis.html.

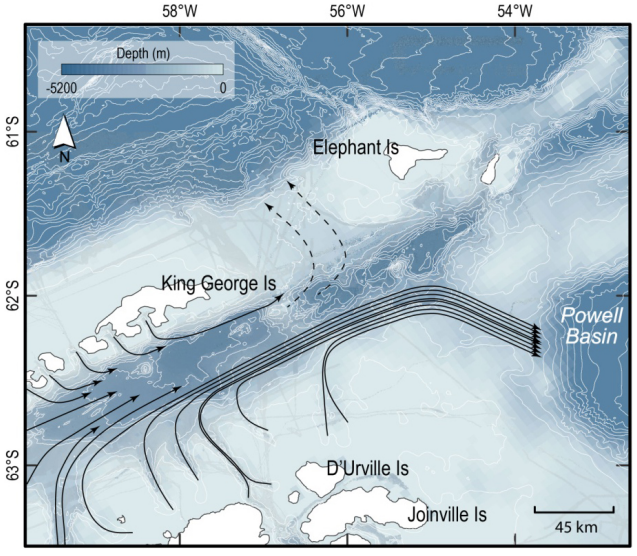

Figure 6. Seabed morphology in Bransfield Strait showing the inferred paleo-flow-line trajectories based on the multibeam imagery (black arrows) and assumptions (black dashed arrows). Background image is from BedMap2 (Fretwell et al., 2013); the island coastline is from the British Antarctic Survey (BAS; http://www.add.scar.org/); the bathymetry contour interval of 250 m is from IBCSO (Arndt et al., 2013).

Keeping in mind that there are no surface expressions of seismic stratigraphic boundaries on the shelf interpreted as a LGM ice stream bifurcation (Smith and Anderson, 2009), we provide two possible explanations to explain the flow divergence we observe in the Larsen B embayment. The first explanation is based on the hypothesis of a non-uniform geological framework. The diverging flow could be explained by the southeastward extension of the Seal Nunatak and Robertson Island post-Miocene volcanic sequence, in contact with Mesozoic rocks in the Larsen embayment. We infer from some seismic data (M. Rebesco, personal communication, 2014) the presence of Mesozoic mudrocks similar to the Nordensköld Formation (Jurassic black shale; Reinardy et al., 2011) and Cretaceous sedimentary sequences of Robertson Island within the Larsen B embayment. These are known to have influenced bed deformation within tills derived from them (Reinardy et al., 2011). One hypothesis, therefore, would suggest that the divergence of flow was related to faster flow and was funneled out of the inner Larsen B embayment by a bed that was more easily deformed (mud base) than the higher friction of the sandy volcaniclastic palagonite units that comprise the Seal Nunatak massif. Detailed petrographic analysis of the respective tills could test this hypothesis.

We also consider the pre-determined topography and glacial dynamics that could have split the flow direction on the mid-shelf. The existence of a slightly elevated seabed over the middle shelf could have acted as a prow between the Robertson Trough and Jason Trough, thus causing diverging flow. This hypothesis cannot be fully tested at this time because heavy ice cover in this particular region makes navigation and acquisition of key swath bathymetry very difficult. However, some bathymetric data and seismic profiles from shipboard surveys south of Jason Peninsula do exist (Sloan et al., 1995) and these show evidence of shallow shelf banks at less than 300 m water depth. Such topographic highs could have divided the glacial flow (Fig. 5). The examination of a time series of MODerate-resolution Imaging Spectroradiometer (MODIS) images from the northeastern AP also shows unequivocal evidence of several previously unknown reef and shoal areas based on their influence on sea ice drift and grounding of small icebergs (Table 1, Fig. 7, Supplement S1, and video S2; see also http://nsidc.org/data/iceshelves_

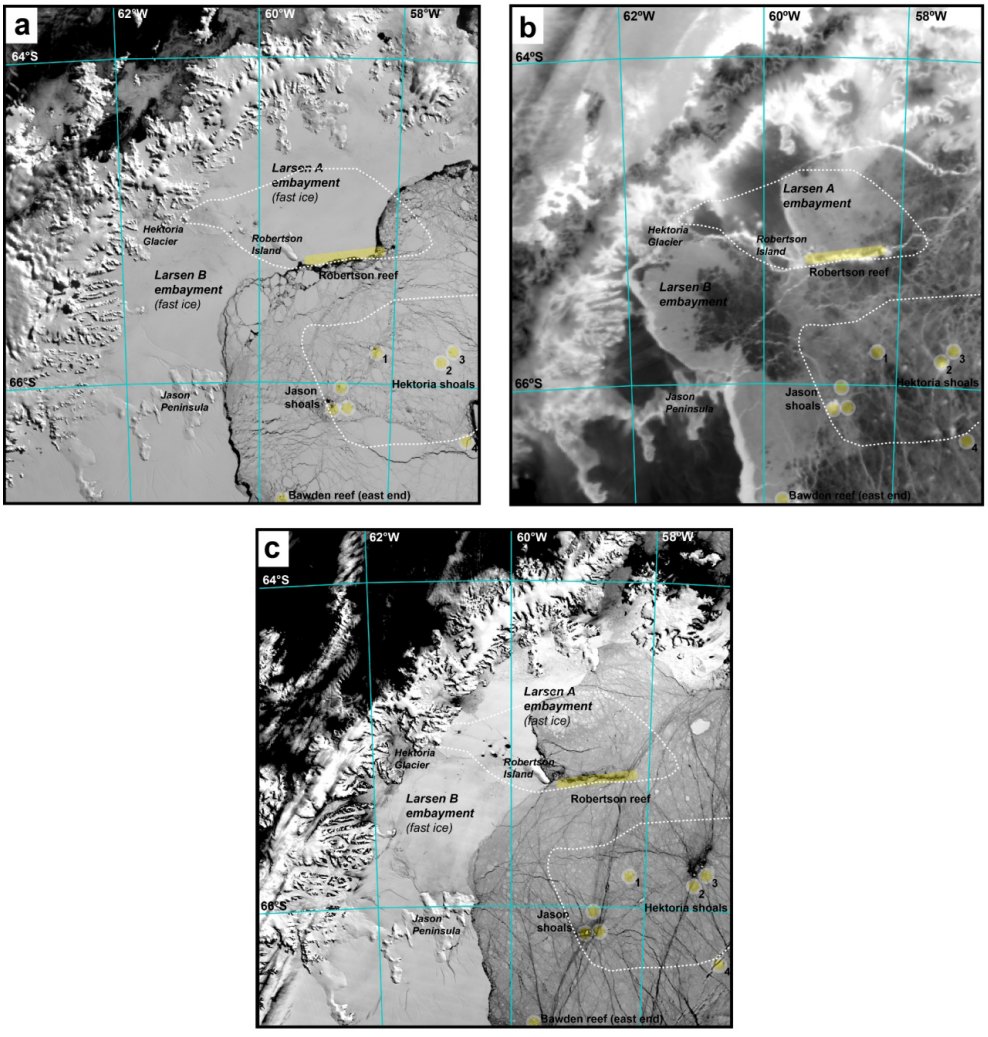

Figure 7. MODerate-resolution Imaging Spectroradiometer (MODIS, 36-band spectrometer) images showing unequivocal evidence of several shoal and reef areas (yellow circle) in the northwestern Weddell Sea, based on sea ice drift and grounding of small icebergs (see also Table 1). The shelf ice domes Hektoria and Robertson are showed in dashed white lines. **(a)** 5 October 2007, band number (BN) 02 (bandwidth 841–876 nm, spatial resolution of 250 m); **(b)** 20 August 2010, BN 32 (bandwidth 11770–12270 nm, spatial resolution of 1000 m); and **(c)** 26 January 2013, BN 02 (bandwidth 841–876 nm, spatial resolution of 250 m).

images/index_modis.html). Luckman et al. (2010) demonstrated the reliability of using satellite remote-sensing tools to identify western Weddell Sea grounded tabular icebergs and to estimate their draft, which they interpreted as maximum water depth. In the 12-year series of images, shoal areas appear as frequent stranding areas of small icebergs, particularly during heavy winter sea ice periods. Larger icebergs (having 200–350 m keels) show drift paths strongly controlled by the shoals. Stranding of icebergs (especially for the informally named Bawden, Robertson, and Jason shoal or reef areas; see Table 1) indicates the shallowest areas of the region. These high areas could have served as centers of glacial nucleation similar to the model proposed for shallows across the Bellingshausen Sea continental shelf (Domack et al., 2006).

The two mechanisms described above could have interacted to cause the divergence of the flow observed from the Larsen B embayment; a process combination of a deformation of weak bed material and a bifurcation of the ice around a topographic high. Divergence of flow lines has been observed at the margin of the Greenland Ice Sheet and Antarctica. A modern example that shows fast-flowing ice bifurcation can be observed on the flow velocity field map of the northeast Greenland Ice Stream, where the southern flow feeds Storstrømmrn and flows into the northern outlet glaciers of Zachariæ Isstrøm and Nioghalvfjerdsfjorden (Joughin et al., 2001, 2010). Modern analogs such as Siple Dome show diverging flow of marine-based ice streams (bed 600 to 700 m b.s.l. – below sea level) around a topographic high only 300 to 400 m b.s.l. (Fretwell et al., 2013). In the

Siple Coast region, only a 200 to 300 m topographic difference is sufficient to create diverging flow separated by ice domes. In addition to these real-world examples, modeling has shown that either a relative topographic high or a relative increase in the basal drag can lead to divergence of ice flow and formation of an elongated ice dome between them. A number of researchers have modeled the surface expression of variability in bed topography or bed properties; a comprehensive analysis is provided by Gudmundsson (2003).

4.2 Evidence of ice divides

We define an ice divide as a boundary separating divergent ice-flow directions, i.e., the line that separates neighboring drainage systems, analogous to a water divide. The separation of the west and east AP along the Bruce Plateau and Detroit Plateau on the Trinity Peninsula and the Graham Land Coast formed the primary ice divide for the AP during LGM. Our results, based on details of the ice-flow directions and modern subaerial and submarine topography, suggest that secondary ice divides split off from the primary ice divide creating several large draining basins (Fig. 5). On the eastern side of the peninsula, we define four major ice divides:

1. from the AP across the Seal Nunatak and Robertson Island to divide the ice flow between the northeast Larsen B embayment and the western area of Larsen A;
2. from the Bruce Plateau (AP) to Cape Longing to divide flows between Larsen A and southern Prince Gustav Channel;
3. from the Detroit Plateau (AP) southeast across the Prince Gustav Channel and up across the center of James Ross Island (Camerlenghi et al., 2001), before continuing across Admiralty Sound and Seymour Island to split the ice flow between the southern and northern Prince Gustav Channel, dividing the ice flow on James Ross Island and Admiralty Sound; and
4. from the Trinity Peninsula to the Joinville Island Group and along the axis of D'Urville Island, across the Larsen Channel, Joinville Island, and Dundee Island according to the seabed morphology in the Antarctic Sound.

On the western AP, the boundary of major ice divides runs

1. along the South Shetland archipelago;
2. from the AP across the Orleans Strait, Trinity Island, and along a series of shelf banks at the western end of the Bransfield Strait that divide the ice flow between the Bransfield Strait and Gerlache–Boyd Strait;
3. from the Bruce Plateau (AP) across Gerlache Strait, Wiencke Island, the southern edge of Anvers Island, Schollaert Channel, and up along the crest of Brabant Island to explain the constriction of flow lines in the Gerlache Strait; and
4. along Anvers Island and Renaud Island to explain the Palmer Deep and Hugo Island Trough ice-flow system and its separation from the Biscoe Trough.

Table 2. Continental-shelf domes estimated area and minimum and maximum estimated ice volumes using the simple Bodvarsson–Vialov model (Bueler et al., 2005).

Continental ice dome	Area (km^2)	Ice volume (km^3)	
		Minimum	Maximum
Hugo Dome	13 675	10 000	11 200
Marr Dome	4950	2500	3300
Brabant Dome	12 850	8200	10 200
Livingston Dome	8075	5000	5500
Snow Hill Dome	14 835	10 800	14 000
Robertson Dome	7560	5000	6200
Hektoria Dome	12 920	9300	12 000
Total	74 865	50 800	62 400

Ice divides typically evolve into elongated ice domes with topographic highs that influence the spatial pattern of accumulation rate and the ice-flow directions. These divides are not stationary and can evolve under variations in climate or boundary conditions (e.g., Nereson et al., 1998; Marshall and Cuffey, 2000). Indeed, an entire ice dome can change shape as climate conditions change on a timescale of a few hundred to thousand years, depending on the accumulation rate and size of the divide (Nereson et al., 1998; Marshall and Cuffey, 2000).

4.3 Inferred ice domes on the continental shelf

The existence of two separate shelf ice domes at LGM, one covering the northern AP and the other upon the South Shetland Islands, was suggested by early work that recognized centers of ice accumulation over the highest existing bedrock topography (Banfield and Anderson, 1995; Bentley and Anderson, 1998). Our LGM ice-flow reconstruction of at least six distinct systems across the northern AP continental shelf and evidence of ice divides serves to delineate at least seven broad regions where additional ice domes may have been centered out on the continental shelf. The presence of the domes is required to constrain lateral spreading of each of the paleo-ice-stream outlets and also to explain the observation of radial flow that, in part, converges with flow within several of the paleo ice stream trajectories. We define each of these features here by assigning names associated with the nearest prominent headland for each ice dome; headlands likely provided some axial orientation to the ice dome. These include Hugo Dome, Marr Dome, Brabant Dome, Livingston Dome, Snow Hill Dome, Robertson Dome, and Hektoria Dome (Fig. 5).

The exact dimensions and character of each of these domes is difficult to define because these areas of the con-

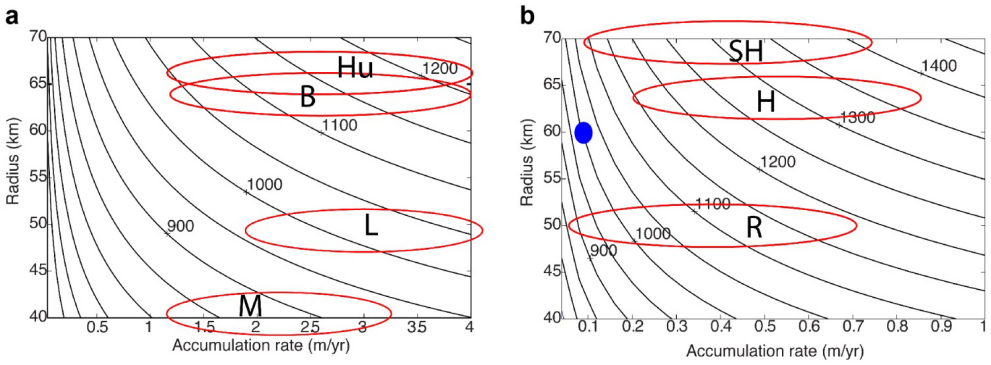

Figure 8. Range of ice thickness expected from **(a)** Marr (M), Livingston (L), Brabant (B), and Hugo (Hu) west AP continental-shelf domes with ice temperature averaging 0 °C and **(b)** Robertson (R), Hektoria (H), and Snow Hill (SH) east AP continental-shelf domes with ice averaging −20 °C using the Bodvarsson–Vialov model (Bueler et al., 2005). The blue dot is the modern analog, 1000 m thick Siple Dome in West Antarctica that fits well the model. See Fig. 5 for the location of the domes.

Table 3. Flow path systems estimated area (continental shelf) and minimum and maximum estimated ice volumes.

Flow path system	Area (km^2)	Approximate length (km)	Ice volume (km^2)	
			Minimum	Maximum
Biscoe Trough	4625	125	2842	4254
Palmer Deep and Hugo Island Trough	15 000	230	9570	17 255
Barbant	850	60	564	719
Gerlache–Croker–Boyd straits	10 675	300	9234	16 402
South Bransfield Strait streams	5600	110	4211	5834
Erebus–Terror	7125	190	3905	6935
Robertson Trough	18 300	330	13 066	26 149
Larsen B embayment	10 700	217	6736	11 937
Total	72 875	1562	50 128	89 485

tinental shelf are generally devoid of multibeam coverage. Furthermore, extensive iceberg scouring across these banks has largely obscured original glacial flow indicators, which might have provided some sense of paleo-ice-flow direction. Nevertheless, some small troughs and lineated features do exist for at least three of the inferred domes. For the Marr, Brabant, and Livingston domes some radial flow indicators can be seen in small troughs that drain the mid-point divides in about the middle of the continental shelf (Fig. 5). Furthermore, the Hugo Dome can be seen to have directed flow into the Biscoe Trough from a position considerably far out on the continental shelf. Hence, this evidence does indicate that the mid-shelf hosted ice domes as centers of ice accumulation which contributed ice drainage contemporaneous with the large paleo ice streams (Fig. 5). In this hypothesis, the continental-shelf ice domes do not necessarily require excessive elevation, only sufficient height to have grounded the system and allowed each dome to constrain the surrounding paleo-ice streams. Our hypothesis for these ice domes is not without precedent; some work on the East Antarctic margin has postulated a similar situation, where major divides were diverted and constrained by large ice domes that rested upon shelf banks (Eittreim et al., 1995). Also, an independent ice dome centered over the west of the Alexander Island, western AP, persisted through the LGM and deglaciation (Graham and Smith, 2012). Furthermore, there are existing modern ice domes that separate fast-flowing, marine-based ice in West Antarctica, including Siple Dome (with surface elevation of 600 m a.s.l. and an ice thickness of 1000 m; Gades et al., 2000; Conway et al., 2002).

The seaward extent of each of the shelf ice domes would seem to correspond to the outer continental shelf, as outlet systems are uniformly constrained out to the grounding line position (the outer shelf) in each of the systems we examined. The exception to this is the broad apron of the grounding line associated with the Gerlache–Croker–Boyd Strait and Biscoe ice streams. In those cases diverging flow is clearly imaged out across the continental-shelf break, indicating spreading flow toward the grounding line. Indeed, the extensive relief of Smith Island (maximum elevation of 2100 m a.s.l.) would likely have blocked any ice flow associated with the Brabant Dome from reaching the outermost shelf (Fig. 5). This

spreading flow is similar to that observed for unrestricted paleo-ice-stream fans such as in the Kveithola Trough off Svalbard (Rebesco et al., 2011).

While the areal dimensions of the ice domes are fairly certain, their thickness is less well defined. We can assume that these features were thick enough to have served as effective lateral constraints to ice stream outlets and to have allowed the dome to have been grounded across a bathymetry of approximately 350 m on average. The thickness of an ice dome in steady state depends on the regional accumulation rate average, the temperature of the ice, and the aerial extent of the dome outlined in Sect. 2.3 (Bueler et al., 2005). Figure 8 shows the results of our model with red ellipses defining the range of possible ice thickness values for each dome. We assume that the western-side domes (Marr, Livingston, Brabant, and Hugo) have an average ice temperature of 0 °C (Fig. 8a), while the eastern-side domes have an average ice temperature of −20 °C (Fig. 8b). The colder ice is stiffer, which can result in thicker domes when all other parameters are the same. The minor axis of the red ellipses shows a possible range of error in the ice radius associated with the irregular aerial extent of the real ice dome.

For accumulation rates, we base our assumptions on the modern AP, which has a strong orographic precipitation gradient that ranges from $4\,\mathrm{m\,yr^{-1}}$ on the western side to less than $0.1\,\mathrm{m\,yr^{-1}}$ on the eastern side. High accumulation sites will result in thicker ice domes if all other parameters are equal. In the LGM case, the distribution of domes will create multiple precipitation highs and lows as each dome creates its own pattern of orographic precipitation (Roe and Lindzen, 2001). Therefore, we predict the highest accumulation rates for Brabant, Livingston, and Hugo Domes. Marr Dome will likely be shielded somewhat from the highest accumulation. On the eastern side, Hektoria and Snow Hill Domes are likely to have slightly higher accumulation than Robertson Dome, as they may receive some precipitation from the Weddell Sea. We have selected a broad range of accumulation rates because we have only general atmospheric patterns from which to draw our assumptions. Despite this large range of input values, we can bracket the ice thicknesses for each dome as presented in Fig. 8 and estimate volumes as shown in Table 2.

4.4 Regional implications

We have presented a compilation of paleo-ice-flow indicators for the northern AP and used the resulting map to infer ice-flow patterns, ice divides, and ice domes. This allows an integrated view over the full extent of the APIS at the LGM. This mapping effort suggests that the seabed topography and the complex geology influenced the ice-flow route and regime at the LGM. The bifurcation of the flow lines in the Larsen B embayment affected the character of the basal ice erosion mechanisms. In general, diverging ice flow is associated with an area of decelerating flow (e.g., Stokes and Clark, 2003). Moreover, the increased flux of ice and debris flowing around a topographic high could provide a powerful feedback where an ice stream could deepen existing depressions (Knight et al., 1994). However, the flow convergences (strongest near the mid-shelf in the northern AP) led to an increase in flow speed at the mid- and upper end of the ice streams, promoting high basal shear stress and significant basal sediment transport (e.g., Boulton, 1990).

It should also be kept in mind that the ice stream catchments include deep basins (i.e., Palmer Deep) that serve as deposystems for thick interglacial mud and ooze deposits. For instance, typical thicknesses for Holocene mud within the Palmer Deep are about 100 m, while across the broader shelf the interglacial muds are no more than 6–8 m thick. This mud could serve as basal lubrication as ice systems advance out across the shelf and eventually ground within the deep inner shelf, thus enhancing streaming flow within the trough trajectory via bed deformation. Once ice streaming was initiated in areas where interglacial sediments provided lubrication, the interglacial sediment would be completely removed by ice; streaming would continue, having been established through regional flow patterns, by eroding the underlying bedrock for more lubricating material and thus enhancing the focus of the trough through multiple cycles.

The presence of multiple APIS ice domes centered on the mid-shelf implies that ice thickness was not uniform on the northern AP continental shelf during the maximum extension of the APIS at LGM. These domes may have harbored significant ice volume above buoyancy, even under minimal scenarios of ice thickness due to their large areal extent. Comparing the estimated total area of the ice domes with the one estimated for the flow paths (Tables 2 and 3) shows that the ice domes were at least as important, if not more so, as the paleo-ice streams, in terms of areal coverage. The minimum estimate for total ice volume of the domes and the paleo-ice streams are similar. However, because the convergent flow paths have significantly deeper beds (as they flow in troughs) the ice streams contain 43 % more maximum ice than the domes.

The presence of multiple ice domes on the shelf would have influenced the ice sheet dynamics (e.g., basal melting and sliding parameters) and the sediment transport to beyond the margin of the ice. The ice velocity would have been slower near the ice divides with lower sediment transport rates than at the peripheral regions where the domes fed out into fast-flowing ice streams with high sediment transport rates. Because of feedbacks between ice dome formation and the orographic precipitation, all of these domes may not have reached their largest extent at the same time; the growth of one dome may "starve" another of its accumulation (e.g., Roe and Lindzen, 2001).

Finally, the delineation of ice domes and faster-flowing outlets is important because it would help to gauge the relative contribution of each system to post-glacial eustatic rise in sea level or, conversely, how each system might have responded to a eustatic or ocean-climate event. For instance,

recent models for glacial recession within the Palmer Deep and along the East Antarctic margin suggest a calving bay re-entrant model, wherein ice streams retreat preferentially landward thus creating a linear "fjord-like" bay surrounded by slower-flowing ice of the domes (Domack et al., 2006; Leventer et al., 2006). This model and others (i.e., Kilfeather et al., 2011) deserve consideration in that our reconstruction clearly outlines differences in the boundary conditions of flow, thickness, bed character, accumulation, and ice sourcing for the domes and converging flow systems. Thus the two systems would logically be expected to respond differently to any forcing factors involved in deglaciation.

The identification of ice domes, ice divides, and diverging/converging flows help us to understand ice-sheet evolution and processes. While considerable effort has been put forward recently toward understanding the character and timing of the retreat of the APIS, more work needs to focus on the reconstruction and detailed vitality of the APIS during the last glacial cycle. The features we recognize have important implications for this effort and the future siting of ice cores and marine drilling sites. Finally, they provide important constraints for glaciohydrology, past and future ice-sheet modeling used, for instance, to look at sediment fluxes (Golledge et al., 2013) or provide more realistic predictions, ice-sheet modeling in response to changing environments, and sea level modeling. The existing challenge includes arranging models of ice-flow and geological data so that they resemble each other, especially when geological features are small compared to the grid scale of ice-flow paths. While the evidence for the ice domes out on the shelf is largely circumstantial, there likely exists today remnants of these features as is the case for the ice cap on Hugo Island, which stands as a prominent feature in the middle of the AP continental shelf.

5 Conclusions

Our results provide considerable improvement in the assessment of ice flow and thereby the dynamics that may have governed the expansion, stabilization, and eventual demise of the ice mass which comprised the APIS. We now not only recognize six spatially defined paleo-ice streams but we can also infer with some confidence the source areas and number of tributaries which fed them. In addition, our study highlights the need to understand the extent and behavior of seven large shelf ice domes that best explain the configuration of the ice-flow directions and serve as lateral constraints to the paleo-ice-stream flow. These ice domes had slower-flowing ice and were likely frozen to their beds, exhibiting somewhat different behavior from the paleo-ice streams which were fed almost exclusively from convergence of tributary glaciers draining the elevated spine of the AP and surrounding islands. Also, while the timing of paleo-ice-stream recession is known in a general way from recent syntheses (Ó Cofaigh et al., 2014), the detailed rates and step backs are far from resolved. Our reconstruction allows focus on the varying character of each ice stream and how this might have influenced differential response to the forcing factors (i.e., eustasy, atmospheric and ocean temperature) and accumulation rates which may have induced instability in the region (Livingstone et al., 2012).

Future research including strategic multibeam coverage, marine sediment cores, and modeling considering the glacio-isostatic rebound are needed to confirm the existence of the ice domes, define their characteristics, and constrain the timing of their ice retreat. When combined with high-resolution dating efforts, our flow reconstruction will help elucidate the retreat history of the ice sheet and, therefore, those forces that acted to destabilize the system and initiate the most recent deglaciation of the APIS.

The Supplement related to this article is available online at doi:10.5194/tc-9-613-2015-supplement.

Acknowledgements. This work was funded by US National Science Foundation grants OPP-0732467 to Eugene W. Domack, ANT-1340261 and ANT-0732921 to Ted Scambos, and OPP-0855265 to Erin C. Pettit and by the Korean Polar Research Institute (PP14010). In addition, we thank the captains and crews of the RVIB *Nathaniel B. Palmer*, *Polarstern*, RRS *James Clark Ross*, BIO *Hesperide*s, and *Araon* and support staff and scientific parties who participated in cruises. This work contains public sector information, licensed under the Open Government Licence v2.0, from the United Kingdom Hydrographic Office for the data collected on HMS *Endurance*, HMS *Scott*, and HMS *Protector*. We thank all principal investigator owners of the released swath multibeam data from the Marine Geoscience Data System portal hosted by Lamont-Doherty Earth Observatory of Columbia University (http://www.marine-geo.org/index.php). C. L. was supported by "TALENTS" Marie Curie COFUND FP7 Programme and an individual research assistant contract within the project MARES-Sustainable Use of Marine Resources (CENTRO-07-ST24-FEDER-002033), co-financed by QREN, Mais Centro – Programa Operacional Regional do Centro e União Europeia/European Regional Development Fund (EU). We wish to thank the reviewers (Mike Bentley and Phil O'Brien) for very helpful reviews of the Discussion version of this manuscript.

Edited by: C. R. Stokes

References

Amblas, D., Urgeles, R., Canals, M., Calafat, A. M., Robesco, M., Camerlenghi, A., Estrada, F., De Batist, M., and Hughes-Clarke, J. E.: Relationship between continental rise development and palaeo-ice sheet dynamics, Northern Antarctic Peninsula Pacific margin, Quaternary Sci. Rev., 25, 933–944, 2006.

Andrews, J. T.: On the reconstruction of pleistocene ice sheets: a review, Quaternary Sci. Rev., 1, 1–30, 1982.

Arndt, J. E., Schenke, H. W., Jakobsson, M., Nitsche, F. O., Buys, G., Goleby, B., Rebesco, M., Bohoyo, F., Hong, J., Black, J., Greku, R., Udintsev, G., Barrios, F., Reynoso-Peralta, W., Taisei, M., and Wigley, R.: The International Bathymetric Chart of the Southern Ocean (IBCSO) Version 1.0 – a new bathymetric compilation covering circum-Antarctic waters, Geophys. Res. Lett., 40, 3111–3117, 2013.

Banfield, L. A. and Anderson, J. B.: Seismic facies investgation of the late Quaternary glacial history of Bransfield Basin, Antarctica, in: Geology and Seismic Stratigraphy of the Antarctic Margin, edited by: Cooper, A. K., Barker, P. F., and Brancolini, G., Antarct. Res. Ser. 68, American Geophysical Union, Washington, D.C., 123–140, 1995.

Barker, P. F.: The Cenozoic subduction history of the Pacific margin of the Antarctic Peninsula: ridge crest-trench interactions, J. Geol. Soc., 139, 787–801, 1982.

Bentley, M. J. and Anderson, J. B.: Glacial and marine geological evidence for the ice sheet configuration in the Weddell Sea-Antarctic Peninsula region during the Last Glacial Maximum, Antarct. Sci., 10, 309–325, 1998.

Boulton, G. S.: Sedimentary and sea level changes during glacial cycles and their control on glacimarine facies architecture, in: Glacimarine Environments: Processes and Sediments, edited by: Dowdeswell, J. A. and Scourse, J. D., Geological Society Special Publication 53, The Geological Society, London, 15–52, 1990.

Brisbourne, A. M., Smith, A. M., King, E. C., Nicholls, K. W., Holland, P. R., and Makinson, K.: Seabed topography beneath Larsen C Ice Shelf from seismic soundings, The Cryosphere, 8, 1–13, doi:10.5194/tc-8-1-2014, 2014.

Bueler, E., Lingle, C. S., Kallen-Brown, J. A., Covey, D., and Bowman, L. N.: Exact solutions and verification of numerical models for isothermal ice sheets, J. Glaciol., 51, 291–306, 2005.

Camerlenghi, A., Domack, E. W., Rebesco, M., Gilbert, R., Ishman, S., Leventer, A., Brachfeld, S., and Drake, A.: Glacial morphology and post-glacial contourites in northern Prince Gustav Channel (NW Weddell Sea, Antarctica), Mar. Geophys. Res., 22, 417–443, 2001.

Canals, M., Urgeles, R., and Calafat, A. M.: Deep sea-floor evidence of past ice streams off the Antarctic Peninsula, Geology, 28, 31–34, 2000.

Canals, M., Casamor, J. L., Urgeles, R., Calafat, A. M., Domack, E. W., Baraza, J., Farran, M., and De Batist, M.: Seafloor evidence of a subglacial sedimentary system off the northern Antarctic Peninsula, Geology, 30, 603–606, 2002.

Canals, M., Calafat, A. M., Camerlenghi, A., De Batist, M., Urgeles, R., Farran, M., Geletti, R., Versteeg,W., Amblas, D., Rebesco, M., Casamor, J. L., Sànchez, A., Willmott, V., Lastras, G., and Imbo, Y.: Uncovering the footprint of former ice streams off Antarctica, EOS, 84, 97–108, 2003.

Clark, C. D.: Mega-sclae glacial lineations and cross-cutting ice-flow landforms, Earth Surf. Proc. Land., 18, 1–29, 1993.

Clark, C. D., Tulaczyk, S., Stokes, C. R., and Canals, M.: A groove-ploughing theory for the production of mega-scale glacial lineations, and implications for ice-stream mechanics, J. Glaciol., 49, 240–256, 2003.

Conway, H., Catania, G., Raymond, C. F., and Gades, A. M.: Switch of flow direction in an Antarctic ice stream, Nature, 419, 465–467, 2002.

Cuffey, K. M. and Paterson, W. S. B. (Eds.): The Physics of Glaciers, Elsevier Inc., Oxford, UK, 2010.

Curry, P. and Pudsey, C. J.: New Quaternary sedimentary records from near the Larcen C and former Larsen B ice shelves; evidence for Holocene stability, Antarct. Sci., 19, 355–364, 2007.

Davies, B. J., Hambrey, M. J., Smellie, J. L., Carrivick, J. L., and Glasser, N. F.: Antarctic Peninsula Ice Sheet evolution during the Cenozoic Era, Quaternary Sci. Rev., 31, 30–66, 2012.

Domack, E. W., Canals, M., Camerlenghi, A., Gilbert, R., Amblas, D., Wilmott, V., Calafat, A. M., Urgeles, R., DeBatist, M., Casamor, J. L., and Rebesco, M.: Complete swath map coverage of the Gerlache Boyd Strait paleo ice stream: an example of collaborative seafloor mapping in the Antarctic Peninsula, XXVIII SCAR Open Science Conference, Bremen, Germany, 26–28 July 2004, Abstract S11/P08, 2004.

Domack, E., Duran, D., Leventer, A., Ishman, S., Doane, S., McCallum, S., Amblas, D., Ring, J., Gilbert, R., and Prentice, M.: Stability of the Larsen B ice shelf on the Antarctic Peninsula during the Holocene epoch, Nature, 436, 681–685, 2005.

Domack, E., Amblas, D., Gilbert, R., Brachfeld, S., Camerlenghi, A., Robesco, M., Canals, M., and Urgeles, R.: Subglacial morphology and glacial evolution of the Palmer deep outlet system, Antarctic Peninsula, Geomorphology, 75, 125–142, 2006.

Dowdeswell, J. A., Ottesen, D., Evans, J., Ó Cofaigh, C., and Anderson, J. B.: Submarine glacial landforms and rates of ice-stream collapse, Geology, 26, 819–822, 2008.

Eittreim, S. L., Cooper, A. K., and Wannesson, J.: Seismic stratigraphic evidence of ice-sheet advances on the Wilkes Land margin of Antarctica, Sediment. Geol., 96, 131–156, 1995.

Evans, J., Dowdeswell, J. A., and Ó Cofaigh, C.: Late Quaternary submarine bedforms and ice-sheet flow in Gerlache Strait and on the adjacent continental shelf, Antarctic Peninsula, J. Quaternary Sci., 19, 397–407, 2004.

Evans, J., Pudsey, C. J., Ó Cofaigh, C., Morris, P., and Domack, E. W.: Late Quaternary glacial history, flow dynamics and sedimentation along the eastern margin of the Antarctic Peninsula Ice Sheet, Quaternary Sci. Rev., 24, 741–774, 2005.

Fretwell, P., Pritchard, H. D., Vaughan, D. G., Bamber, J. L., Barrand, N. E., Bell, R., Bianchi, C., Bingham, R. G., Blankenship, D. D., Casassa, G., Catania, G., Callens, D., Conway, H., Cook, A. J., Corr, H. F. J., Damaske, D., Damm, V., Ferraccioli, F., Forsberg, R., Fujita, S., Gim, Y., Gogineni, P., Griggs, J. A., Hindmarsh, R. C. A., Holmlund, P., Holt, J. W., Jacobel, R. W., Jenkins, A., Jokat, W., Jordan, T., King, E. C., Kohler, J., Krabill, W., Riger-Kusk, M., Langley, K. A., Leitchenkov, G., Leuschen, C., Luyendyk, B. P., Matsuoka, K., Mouginot, J., Nitsche, F. O., Nogi, Y., Nost, O. A., Popov, S. V., Rignot, E., Rippin, D. M., Rivera, A., Roberts, J., Ross, N., Siegert, M. J., Smith, A. M., Steinhage, D., Studinger, M., Sun, B., Tinto, B. K., Welch, B. C., Wilson, D., Young, D. A., Xiangbin, C., and Zirizzotti, A.: Bedmap2: improved ice bed, surface and thickness datasets for

Antarctica, The Cryosphere, 7, 375–393, doi:10.5194/tc-7-375-2013, 2013.

Gades, A., Raymond, C. F., Conway, H., and Jacobel, R.: Bed properties of Siple Dome and adjacent ice streams, West Antarctica, inferred from radio-echo sounding measurements, J. Glaciol., 46, 88–94, 2000.

Gilbert, R., Domack, E. W., and Camerlenghi, A.: Deglacial history of the Greenpeace Trough: ice Sheet to Ice Shelf transition in the Northwestern Weddell Sea, Antarct. Res. Ser., 79, 195–204, 2003.

Glasser, N. F., Davies, B. J., Carrivick, J. L., Rodés, A., Hambrey, M. J., Smellie, J. L., and Domack, E.: Ice-stream initiation, duration and thinning on James Rosse Island, northern Antarctic Peninsula, Quaternary Sci. Rev., 86, 78–88, 2014.

Golledge, N. R., Levy, R. H., McKay, R. M., Fogwill, C. J., White, D. A., Graham, A. G. C., Smith, J. A., Hillenbrand, C.-D., Licht, K. J., Denton, G. H., Ackert Jr., R. P., Maas, S. M., and Hall, B. L.: Glaciology and geological signature of the Last Glacial Maximum Antarctic ice sheet, Quaternary Sci. Rev., 78, 225-247, 2013.

Graham, A. G. C. and Smith, J. A.: Palaeoglaciology of the Alexander Island ice cap, western Antarctic Peninsula, reconstructed from marine geophysical and core data, Quaternary Sci. Rev., 35, 63–81, 2012.

Gudmundsson, G. H.: Transmission of basal variability to a glacier surface, J. Geophys. Res.-Solid Earth, 108, ETG 9-1–19, 2003.

Heroy, D. C. and Anderson, J. B.: Ice-sheet extent of the Antarctic Peninsula region during the Last Glacial Maximum (LGM) – insights from glacial geomorphology, Geol. Soc. Am. Bull., 117, 1497–1512, 2005.

Johnson, J. S., Bentley, M. J., Roberts, S. J., Binnie, S. A., and Freeman, S. P. H. T.: Holocene deglacial history of the northeast Antarctic Peninsula – a review and new chronological constraints, Quaternary Sci. Rev., 30, 3791–3802, 2011.

Joughin, I., Fahnestock, M., MacAyeal, D. R., Bamber, J. L., and Gogineni, P.: Observation and analysis of ice flow in the largest Greenland ice stream, J. Geophys. Res., 106, 34021–34034, 2001.

Joughin, I., Smith, B. E., Howat, I. M., Scambos, T., and Moon, T.: Greenland flow variability from ice-sheet-wide velocity mapping, J. Glaciol., 56, 415–430, 2010.

Kilfeather, A. A., ÓCofaigh, C., Lloyd, J. M., Dowdswell, J. A., Xu, S., and Moreton, S. G.: Ice-stream retreat and ice-shelf history in Marguerite Trough, Antarctic Peninsula: Sedimentological and foraminiferal signatures, Geol. Soc. Am. Bull., 123, 997–1015, 2011.

Knight, P. G., Sugden, D. E., and Minty, C. D.: Ice flow around large obstacles as indicated by basal ice exposed at the margin of the Greenland ice sheet, J. Glaciol., 40, 359–367, 1994.

Larter, R. D. and Barker, P. F.: Seismic stratigraphy of the Antarctic Peninsula Pacific margin: a record of Pliocene–Pleistocene ice volume and paleoclimate, Geology, 17, 731–734, 1989.

Larter, R. D. and Vanneste, L. E.: Relict subglacial deltas on the Antarctic Peninsula outer shelf, Geology, 23, 33–36, 1995.

Lawver, L. A., Sloan, B. J., Barker, D. H. N., Ghidella, M. E., von Herzen, R. P., Keller, R. A., Klinkhammer, G. P., and Chin, C. S.: Distributed, active extension in Bransfield Basin, Antarctic Peninsula: evidence from multibeam bathymetry, GSA Today, 6, 1–6, 1996.

Leventer, A., Domack, E., Dunbar, R., Pike, J., Stickley, C., Maddison, E., Brachfield, S., Manely, P., and McClennan, C.: Marine sediment record from East Antarctica margin reveals dynamics of ice-sheet recession, GSA Today, 16, 4–10, 2006.

Livingstone, S. J., Ó Cofaigh, C., Stokes, C. R., Hillenbrand, C. D., Vieli, A., and Jamieson, S. S. R.: Antarctic palaeo-ice streams, Earth-Sci. Rev., 111, 90–128, 2012.

Luckman, A., Padman, L., and Jansen, D.: Persistent iceberg groundings in the western Weddell Sea, Antarctica, Remote Sens. Environ., 114, 385–391, 2010.

Marshall, S. J. and Cuffey, K. M.: Peregrinations of the Greenland Ice Sheet divide in the last glacial cycle: implications for central Greenland ice cores, Earth Planet. Sc. Lett., 179, 73–93, 2000.

Nereson, N. A., Hindmarsh, R. C. A., and Raymond, C. F.: Sensitivity of the divide position at Siple Dome, West Antarctica, to boundary forcing, Ann. Glaciol., 27, 207–214, 1998.

Nývlt, D., Košler, J., Mlčoch, B., Mixa, P., Lisá, L., Bubík, M., and Hendriks, B. W. H.: The Mendel Formation: Evidence for Late Miocene climatic cyclicity at the northern tip of the Antarctic Peninsula, Palaeogeogr. Palaeoclimatol. Palaeoecol., 299, 363–384, 2011.

Ó Cofaigh, C., Davies, B. J., Livingstone, S. J., Smith, J. A., Johnson, J. S., Hocking, E. P., Hodgson, D. A., Anderson, J. B., Bentley, M. J., Canals, M., Domack, E., Dowdeswell, J. A., Evans, J., Glasser, N. F., Hillenbrand, C. D., Larter, R. D., Roberts, S. J., and Simms, A. R.: Reconstruction of ice-sheet changes in the Antarctic Peninsula since the Last Glacial Maximum, Quaternary Sci. Rev., 100, 87–110, 2014.

Pudsey, C. J., Barker, P. F., and Larter, R. D.: Ice Sheet retreat from the Antarctic Peninsula shelf, Cont. Shelf. Res., 14, 1647–1675, 1994.

Pudsey, C. J., Evans, J., Domack, E. W., Morris, P., and Del Valle, R. A.: Bathymetry and acoustic facies beneath the former Larsen-A and Prince Gustav ice shelves, north-west Weddell Sea, Antarct. Sci., 13, 312–322, 2001.

Rebesco, M., Liu, Y., Camerlenghi, A., Winsborrow, M., Laberg, J. S., Caburlotto, A., Diviacco, P., Accettella, D., Sauli, C., Wardell, N., and Tomini, I.: Deglaciation of the western margin of the Barents Sea Ice Sheet – a swath bathymetric and sub-bottom seismic study from the Kveithola Trough, Mar. Geol., 279, 141–147, 2011.

Rebesco, M., Domack, E., Zgur, F., Lavoie, C., Leventer, A., Brachfeld, S., Willmott, V., Halverson, G., Truffer, M., Scambos, T., Smith, J., and Pettit, E.: Boundary condition of grounding lines prior to collapse, Larsen-B Ice Shelf, Antarctica, Nature, 345, 1354–1358, 2014.

Reinardy, B. T. J., Larter, L. D., Hillenbrand, C. D., Murray, T., Hiemstra, J. F., and Booth, A. D.: Streaming flow of an Antarctic Peninsula palaeo-ice stream, both by basal sliding and deformation of substrate, J. Glaciol., 57, 596–608, 2011.

Roe, G. H. and Lindzen, R. S.: The mutual interaction between continental-scale ice sheets and atmospheric stationary waves, J. Climate, 14, 1450–1465, 2001.

Scambos, T. A., Hulbe, C. L., and Fahnestock, M.: Climate-induced ice shelf disintegration in the Antarctic Peninsula, in: Antarctic Peninsula Climate Variability, edited by: Domack, E. W., Leventer, A., Burnett, A., Bindschadler, R., Convey, P., and Kirby, M., Antarct. Res. Ser. 79, American Geophysical Union, Washington, D.C., 79–92, 2003.

Simms, A. R., Milliken, K. T., Anderson, J. B., and Wellner, J. S.: The marine record of deglaciation of the South Shetland Islands, Antarctica since the Last Glacial Maximum, Quaternary Sci. Rev., 30, 1583–1601, 2011.

Sloan, B. J., Lawver, L. A., and Anderson, J. B.: Seismic stratigraphy of the Larsen Basin Eastern Antarctic Peninsula, in: Geology and Seismic Stratigraphy of the Antarctic Margin, edited by: Cooper, A. K., Barker, P. F., and Brancolini, G., Antarctic Res. Ser. 68, American Geophysical Union, Washington, D.C., 59–74, 1995.

Smith, R. T. and Anderson, J. B.: Ice-sheet evolution in James Ross Basin,Weddell Sea margin of the Antarctic Peninsula: the seismic stratigraphic record, Geol. Soc. Am. Bull., 122, 830–842, 2009.

Smith, T. and Anderson, J. B.: Seismic stratigraphy of the Joinville Platform: implications for regional climate evolution, in: Tectonic, Climatic and Cryospheric Evolution of the Antarctic Peninsula, edited by: Anderson, J. B. and Wellner, J. S., American Geophysical Union Special Publication 063, American Geophysical Union, Washington, D.C., 51–62, 2011.

Stokes, C. R. and Clark, C. D.: The Dubawnt Lake palaeo-ice stream: evidence for dynamic ice sheet behaviour on the Canadian Shield and insights regarding the controls on ice-stream location and vigour, Boreas, 32, 264–279, 2003.

Vanneste, L. E. and Larter, R. D.: Deep-tow boomer survey on the Antarctic Peninsula Pacific Margin: an investigation of the morphology and acoustic characteristics of Late Quaternary sedimentary deposits on the outer continental shelf and upper slope, in: Geology and Seismic Stratigraphy of the Antarctic Margin, Part 1, edited by: Cooper, A. K., Barker, P. F., and Brancolini, G., American Ggophysical Union, Washington, D.C., 97–121, 1995.

Wellner, J. S., Lowe, A. L., Shipp, S. S., and Anderson, J. B.: Distribution of glacial geomorphic features on the Antarctic continental shelf and correlation with substrate: implications for ice behavior, J. Glaciol., 47, 397–411, 2001.

Wellner, J. S., Heroy, D. C., and Anderson, J. B.: The death mask of the antarctic ice sheet: comparison of glacial geomorphic features across the continental shelf, Geomorphology, 75, 157–171, 2006.

Willmott, V., Canals, M., and Casamor, J. L.: Retreat history of the Gerlache–Boyd ice stream, Northern Antarctic Peninsula: an ultra-high resolution acoustic study of the deglacial and postglacial sediment drape, in: Antarctic Peninsula Climate Variability, edited by: Domack, E. W., Leventer, A., Burnett, A., Bindschadler, R., Peter, C., and Kirby, M., Antarct. Res. Ser., 79, 183–194, 2003.